

## Chapter 1:

# Introduction

*“The most important thing is not to stop questioning. Curiosity has its own reason for existing. One cannot help but be in awe when he contemplates the mysteries of eternity, of life, of the marvellous structure of reality.”*

*Albert Einstein*

Porous materials have long been of interest in industrial fields as catalytic supports and adsorbents. Many different types of porous materials have been used in these applications, ranging from activated carbons, to zeolites. More specifically, silica based systems such as clays, silica gels and zeolites have been used in many catalytic processes and adsorption and separation applications. ZSM-5 is used as a catalyst for conversion of natural gas to motor fuel.<sup>1</sup> Zeolites A and X are used in detergents to soften water by removal of calcium and magnesium ions via ion exchange.<sup>1</sup> Porous silica gels have been used in filtration, chromatography, thermal/acoustic insulation, and as desiccants.<sup>2</sup> These, however, each have a range of practical use dictated by the size, shape and selectivity of the pores in the material and each has a distinct manner of preparation to produce the required pore structure. The molecular sieve MCM-41 forms a part of this spectrum of porous, silicate materials. A short comparison with some of these other materials follows.

Silicates are built up from  $[\text{SiO}_4]^{2-}$  tetrahedra. Each tetrahedron is connected to other tetrahedra to form a three dimensional network. They may share from one, up to all four of the oxygen atoms with adjacent tetrahedra. Tetrahedra connected by two atoms form a chain; by three atoms, a sheet; and by four atoms, a three dimensional network.<sup>3</sup> Materials in which all four oxygen atoms in all tetrahedra are shared with other tetrahedra form dense structures such as quartz and cristobalite. In amorphous silica, which is less dense, there is a random packing of tetrahedra in a non-periodic structure in which at least two corners in each tetrahedron are shared. The Si-O-Si angles in these structures may vary, but the silicon-oxygen bond length is constant at around 0.162 nm.<sup>3</sup>

## 1.1 Porous Silicates

Porous silica is generally discussed as a subsection of the larger group of porous aluminosilicate materials. These may be one of two general types. The crystalline form, zeolites, or the less ordered porous silicates and aluminosilicates which include silica gels, and pillared clays. Both contain pores within the bulk material which may host other molecules, allowing interactions with the surface or with other molecules trapped within the structure to take place.

Zeolites are crystalline aluminosilicates where the channel structure may be one or two dimensional. The channels in these materials are part of the crystal lattice of the material, and so are highly monodisperse and have fixed directionality within the crystal. They have a pore size range<sup>1</sup> between about 4 and 7 Å, since the size and shape of these holes is determined by the stability of large rings made up of alternating silicon and oxygen atoms. The widest aperture in conventional aluminosilicate zeolites is a ring of 12 tetrahedral atoms and is 7.4 Å in diameter.<sup>4,5</sup> The uniformity of the channels in zeolitic systems means they are extremely selective adsorbents for small molecules of particular molecular geometries and sizes,<sup>1,6,7</sup> and so make highly selective catalytic supports, and adsorbents. However the narrow range of pore sizes available and the relatively small cross section of those pores restricts the size of molecules which may escape from or enter the pores to access catalytic or adsorption sites. This limits their use in applications involving larger organic molecules. Crystalline materials with larger pores (8-14.5 Å) have been prepared in aluminophosphate systems,<sup>8-10</sup> and are found in the natural ferroaluminophosphate, caxoxenite (14 Å),<sup>11</sup> but again, these materials are apparently limited by the size of void which may be accommodated in a crystalline system.

Porous silica gels are generally prepared via sol-gel methods, in which molecular or colloidal silicate species are dispersed in a solvent, and then form a gel which may lose solvent as the condensation of the silica proceeds. The silica walls in these materials are amorphous, showing no long-range order. The pores in these materials are a result of the process of gelation, which depends upon the reaction conditions (*eg.* temperature, pH), and the solvents and reagents used.<sup>2</sup> Other porous materials include modified layered materials, such as pillared smectite clays and layered double hydroxides, as well as porous glasses. Generally these materials have larger pores than zeolites, but the distribution of pore sizes is also larger, and the pores exist as a disordered network throughout the solid. This lack of uniformity is reflected in a corresponding lack of selectivity in adsorption and catalysis applications. They provide relatively high surface area, inert supports for catalysts, and can be prepared at various densities. Aerogel materials prepared by supercritical drying of wet gels may have densities as low as 0.003 g cm<sup>-3</sup> with porosities of 98%<sup>12</sup> and surface areas of more than 1000 m<sup>2</sup> g<sup>-1</sup>.<sup>2</sup> They are used as Cherenkov detectors in particle physics applications and as window and bulk insulation. It has been suggested aerogels could be used as gas filters or that metal-loaded aerogels could be used as catalyst beds in the petroleum industry.<sup>12</sup> The distribution of pore sizes in these materials is *ca.* 10-500 Å. In xerogels, which are air-dried gels with a surface area of 500-900 m<sup>2</sup> g<sup>-1</sup>, the pore diameters can range from 10-200 Å within the one sample.<sup>2</sup>

The pillaring of layered silicates, such as montmorillonite, hectorite and saponite with intercalates, such as polyoxocations of aluminium, zirconium and chromium, results in materials with Lewis acid sites, provided by coordinately unsaturated metal ions on the pillars.<sup>13</sup> These materials therefore have novel catalytic properties and void volumes which are mostly within the nanoporous range (1.0-10 nm). Layered double hydroxides may be pillared with Keggin and other polyoxometallate ions, or metallo macrocyclic anions. Applications of these pillared materials focus on use as shape-selective heterogeneous catalysts for petroleum cracking, and for use in the treatment of polluted ground waters and industrial effluent.<sup>13</sup> Porous silica glasses, made by etching phase-separated borosilicate glasses prepared from high temperature melts,<sup>2</sup> have been used to measure the effects of confined spaces upon the collective behaviour of molecules adsorbed in the pores,<sup>14</sup> and to provide experimental observations whereby theories of molecular adsorption may be tested. Applications such as these would benefit from a simplified analysis if a material with a monodisperse pore size distribution was used.

## 1.2 MCM-41

The mesoporous molecular sieve, MCM-41 shares characteristics of both types of porous silica. The wall structure of this material appears to be amorphous, with densities close to those of colloidal silica.<sup>15</sup> In X-ray diffraction patterns, no sharp Bragg peaks are seen at angles corresponding to the silicon-oxygen distances observed in crystalline silicates. Instead, a broad hump of scattering is observed, more characteristic of a glass or amorphous silica system.<sup>16,17</sup>

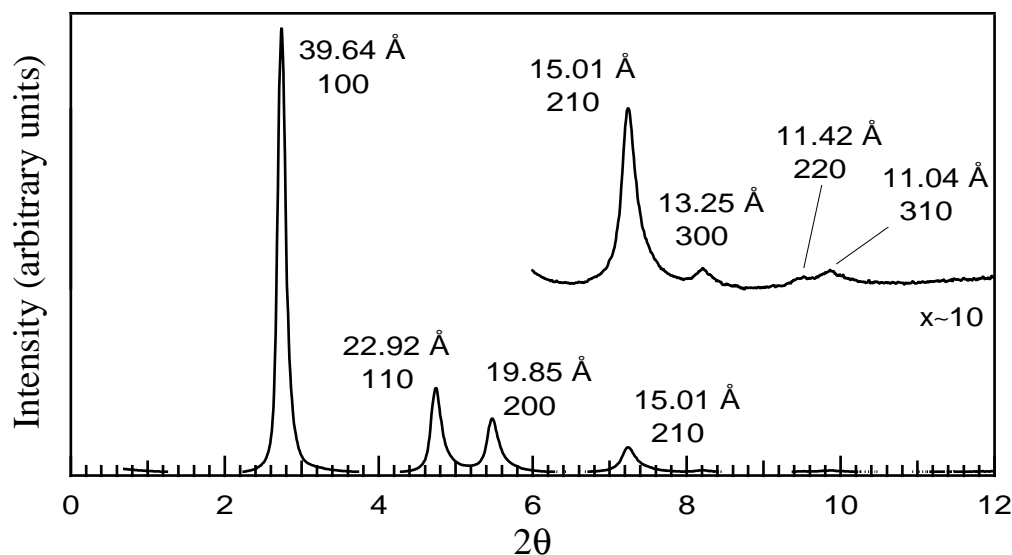


**Figure 1.1** Powder diffraction pattern, showing the intensity versus the scattering angle,  $2\theta$ , for a pure silica MCM-41 material. The inset is the pattern for the last four peaks multiplied by a factor of ten so that they could be shown on the same scale as the first three peaks. The peaks are indexed on a hexagonal lattice in two dimensions, and the d-spacing for each peak are given.

The pore system of MCM-41 within this amorphous framework is, however, very well ordered. The long, cylindrical channels in this material are in a hexagonally close

packed arrangement, which is sufficiently organised for a diffraction pattern to arise from the arrangement of these pores. The pores are large (15-100 Å<sup>18</sup>), in the mesopore range (which is defined as between 20 - 500 Å<sup>19</sup>) which is two to three times those found in crystalline zeolitic systems, and so the repeat distance between channels is much greater than the distances between diffracting layers in crystals.

The X-ray diffraction pattern derives from this large channel repeat distance, rather than any crystalline order in the atoms comprising the walls, and is therefore seen at low angles. The inherent disorder in such an amorphous system may be seen in the rapid decrease in diffraction peak intensity as higher orders of diffraction, at larger angles, are reached. An indexed diffraction pattern of a well-ordered MCM-41 material taken at a high intensity synchrotron X-ray source is shown in Figure 1.1 above. Further discussion of the diffraction methods and instrumentation may be found in Chapter 3.

### 1.3 Templated Systems

Zeolitic materials, with their pores incorporated in a crystalline framework, may occur naturally, but are more often made synthetically by hydrothermal processes. The synthetic methods usually involve the addition of silicate monomers or polymers to pre-existing “seed” crystals,<sup>20</sup> or a nucleation process around an organic template molecule.<sup>21</sup> The presence of a molecular template determines to some extent the size and shape of the pore created in the zeolite, but it forms part of the crystal lattice of the growing zeolite, and so is encapsulated only in certain sites in the crystal. Some zeolites form in the absence of these template molecules, and whether the template has a structure-directing, or merely a space-filling role is dependant upon the particular zeolite and template molecule concerned.<sup>21,22</sup>

There are several competing pathways proposed for the mechanism of zeolite synthesis, which allow for the presence of the template molecule in the condensing silica framework. In all of these however, the driving force for the observed ordering is the condensation of the silica framework. The liquid-phase-ion-transport mechanism<sup>23-25</sup> proposes the formation of composite species in solution, made up of the template molecule surrounded by a loose shell of silica polyanions and water molecules. The structure of these nuclei has been described as clathrate-like,<sup>26</sup> but is probably not sufficiently ordered so as to resemble crystal fragments. Secondary building units comprised of silicon-oxygen rings of various sizes and connectivities, as seen in the structures of fully formed zeolites, have been proposed as one pathway for structure development.<sup>20,27</sup> There is some debate over whether such structures in fact exist in solution, and their role in zeolite nucleation.<sup>28</sup> Knight<sup>29</sup> has described such secondary building units as “red herrings”, preferring to describe the process as the displacement of the ordered sheath of water molecules present around a template molecule by small silicate oligomers. These less ordered oligomers are held in place long enough to allow condensation into partially ordered structures around the template, which then continue condensation with further oligomers in order to nucleate the zeolite.

In the liquid-phase-ion-transport mechanism, these zeolite nuclei both agglomerate during the synthesis process, and draw further silicate species from the reaction solution, or from any precipitated silica gel in the system to assemble the crystalline silica/organic lattice. The solid-hydrogel-reconstruction model<sup>30,31</sup> instead suggests that the template molecule is precipitated along with amorphous silica into a silica gel phase. Within this gel, local re-ordering around each template molecule occurs, with atoms diffusing into place on the crystal lattice. Composite models have also been put forward, in which the zeolite nuclei form in solution and then adhere to the gel phase where further crystal growth occurs.<sup>32-34</sup>

In MCM-41 syntheses, by contrast, the template role is taken not by a *single* molecule but by an *array* of molecules, self-organised into a liquid crystalline phase. The liquid crystal template mechanism differs from that of zeolite formation in that it is not the silicate condensation which is the dominant factor in the formation of the structure. Instead it is the organisation of the surfactant molecules into micellar phases which defines the structure.<sup>18</sup> In support of this mechanism it has been found that in regions of the phase diagram where a surfactant does not form liquid crystal phases, *ie.* for very high temperatures,<sup>35,36</sup> or at concentrations below the critical micelle concentration<sup>5,37</sup> (cmc), addition of silicate does not result in mesoscale structures. At high temperatures porous materials such as ZSM-48, which are templated around a single surfactant molecule are formed, rather than structures based on liquid crystal arrays.<sup>35</sup>

The species first used in mesophase syntheses were quaternary amine surfactants. These are known to form a variety of liquid crystal phases in water by virtue of the interaction of their hydrophilic headgroups and hydrophobic hydrocarbon tails with the polar water phase.<sup>38,39</sup> The surfactant phase which forms in an aqueous solution is dependant upon the surfactant concentration and its counterion. It may be determined by the packing parameter  $v/al$  where  $v$  is the volume of the hydrocarbon chain,  $a$  the headgroup area and  $l$  the maximum effective chain length (somewhat less than the fully extended molecular length of the chain, typically  $l=1.5+1.265n$  Å where  $n$  is the number of carbon atoms in the chain or one less).<sup>40-42</sup> For cylindrical micelles  $1/3 < v/al < 1/2$ , whereas for spherical micelles  $v/al < 1/3$ . The parameter,  $a$ , is known to be sensitive to the surfactant counterion. The packing parameter is essentially a measure of the curvature of the structure formed. Generally, at the lowest concentrations, the surfactant will exist as monomers in solution. With increasing surfactant concentration (for the same counterion) it becomes more energetically favourable to form micelles, which initially are spherical. Spherical micelles contain the largest area per headgroup for any of the surfactant micelle phases. Increasing concentration further raises the aggregation number in the micelle, reduces the area per headgroup, and may result in elongation of the micelle to form a rod in solution. Still further increases in surfactant concentration leads to agglomeration of the micelles, whether spherical or cylindrical, into a close packed phases, which, in the case of rod-like micelles is a hexagonal phase. The next level of concentration gives a cubic phase in which there is one continuous bilayer of surfactant separating two distinct water regions in which the surfactant forms a cubic gyroid minimal surface. The final phase transition is to a lamellar phase, composed of bilayers of surfactant, separated by a water phase. This phase has the least curvature and the smallest area per surfactant headgroup. Figure 1.2 illustrates the

surfactant liquid crystal phases and shows a phase diagram for pure cetyltrimethylammonium bromide, the surfactant used as the template molecule in this work.

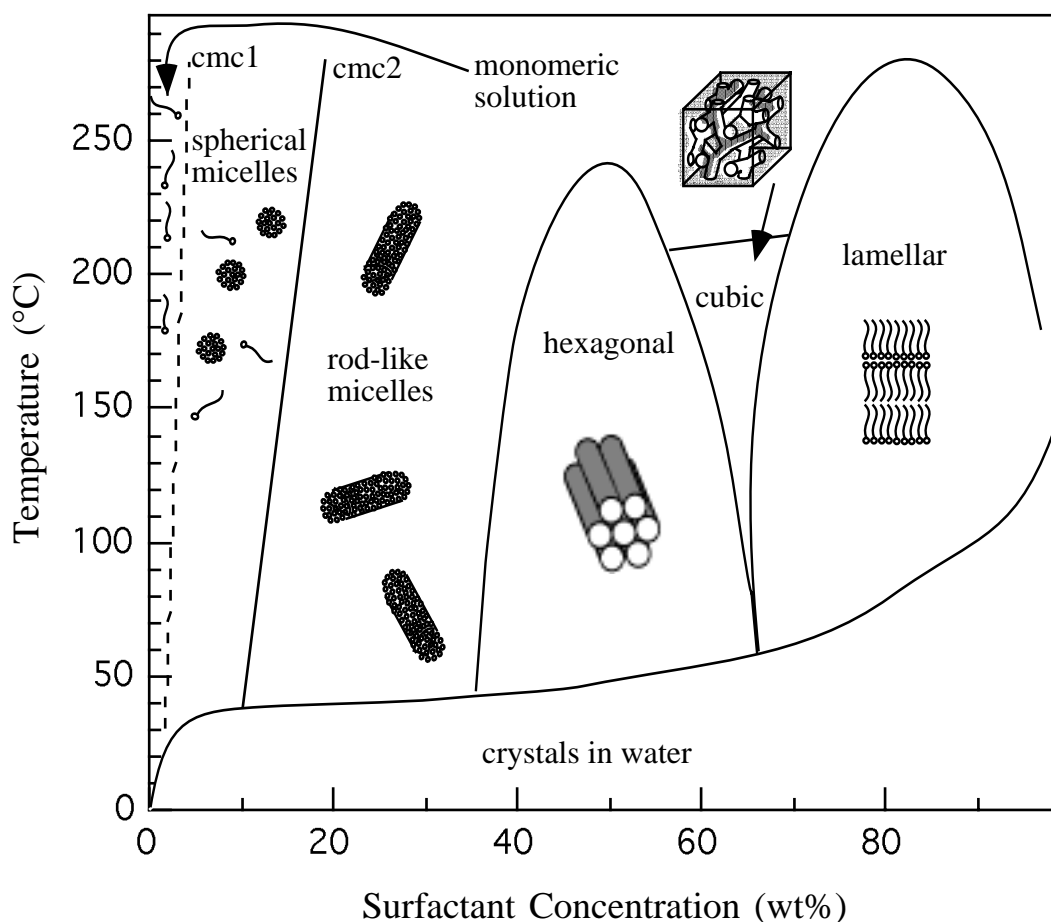


**Figure 1.2** A phase diagram<sup>43</sup> and schematics of the corresponding surfactant liquid crystal phases for the surfactant used as template in this work. *Cmc1* is the critical micelle concentration for the formation of spherical micelles, which has been exaggerated to higher concentrations for the purposes of the illustration. *Cmc2* is the critical micelle concentration for the formation of rod-like micelles.

The MCM-41 material discussed in this work has the same overall structure as the surfactant hexagonal liquid crystal phase. Considerable work has also been carried out on silica/surfactant systems which mimic the other concentrated surfactant liquid crystal phases.<sup>44</sup> Lamellar phases were synthesised by Bull *et al.*<sup>45</sup> and by Dubois *et al.*,<sup>46</sup> who used a double chain surfactant. The lamellar silica/surfactant phase has also been observed as a precursor phase to the formation of the hexagonal phase.<sup>47</sup> The cubic phase was also reported by Beck *et al.*<sup>18</sup> and interconversions between the hexagonal and cubic phase have been observed.<sup>48</sup> More complex systems with multiwalled surfactant vesicles have also formed templates for the formation of patterned spheres,<sup>49,50</sup> and other structures strongly suggestive of silica frameworks formed by diatoms.<sup>51,52</sup> Combinations of the mesoporous system with other structure directing systems has given discrete, large mesoporous silica spheres, grown in an oil-water emulsion<sup>53</sup> and ordered macroporous fibres of mesoporous silica templated around a thread of co-aligned multicellular filaments of *Bacillus subtilis*.<sup>54</sup> The surfactants used

to create mesophase silicates have covered the full range of micelle forming species; cationic, anionic<sup>55</sup> and neutral molecules<sup>56,57</sup> have been used.

## 1.4 The Synthesis of MCM-41

MCM-41 was first reported by researchers from Mobil Oil in 1992.<sup>18,58-61</sup> They reported the formation of the hexagonal phase mesoporous material under a wide range of synthetic conditions. They used temperatures for the hydrothermal synthesis ranging from 25°C to 175°C<sup>61</sup> for periods from 5 minutes to 14 days, at initial pH values of 1-14.<sup>60</sup> Quaternary ammonium surfactants with chain lengths ranging from 8 carbon atoms to 16 were used, and other organic molecules, such as mesitylene, were used to swell the surfactant phases to allow templating of larger pores.<sup>18</sup> A variety of silica sources, from monomeric to highly condensed, and a corresponding variety of alumina sources were investigated.

Since this early work, other authors have commonly used tetraethylorthosilicate (TEOS) as the silica source, and the n-C<sub>16</sub> quaternary ammonium chloride or hydroxide surfactant, although there have also been many other reagents reported in the literature. Notably, a highly ordered hexagonal MCM-41 material has recently been reported by Khushalani *et al.*<sup>62</sup> which was prepared using TEOS and a cetylpyridinium chloride surfactant. Generally it has been found that increasing the degree of condensation of the silica source favours hexagonal phase formation while increasing the initial pH of the synthesis gel favours the lamellar phase.<sup>63</sup> Various post-synthesis treatments have also been applied to increase the long-range order and stability of this material. These include continued heating at 100°C in a water solution with a range of pH values,<sup>48,64</sup> or impregnating with 20% nitric acid at room temperature overnight.<sup>65</sup>

In this work, a relatively simple system was chosen, in order to reduce the number of possible variables. The set of reagents selected (see Chapter 2), and their concentrations (based on a preparation initially published by Beck *et al.*<sup>18</sup>) were taken as standard, and optimisation and investigation of the synthesis restricted to that context only. The factors investigated were: heating/aging time in the gel, the presence or absence of stirring, the pH of the preparation during synthesis, and the effect of the type of acid used to maintain a selected pH. The effect of these factors throughout the synthesis process was examined as well as the structure and stability of the final products.

## 1.5 Mechanism of MCM-41 Formation

The molecular interaction between an inorganic material and a surfactant headgroup can be understood using conventional reaction schemes. Six different possible molecular reaction pathways<sup>57,66,67</sup> which use the principle of liquid crystal templating have been identified: S<sup>+</sup>I<sup>-</sup>, S-I<sup>+</sup>, S<sup>+</sup>X<sup>-</sup>I<sup>+</sup>, S-X<sup>+</sup>I<sup>-</sup>, S-I and S<sup>o</sup>I<sup>o</sup>, where S is the surfactant, I is the inorganic phase, and X is a mediating ion. S-I indicates systems where the inorganic precursor is covalently bonded to the template throughout synthesis, an approach which has been used for some transition metal oxide analogues of MCM-41.<sup>68-70</sup> The pathway applicable to a particular synthesis will be dictated by the reagents and synthetic

conditions and can influence the physical and chemical properties of the product. In this work, the  $S^+I^-$  reaction mechanism is used since the pH used (7 to 12) ensures negatively charged silicate ions, although mesoporous silicates may also be formed via  $S^{\circ}I^{\circ}$  (pH  $\approx$  7) and  $S^+X^-I^+$  (pH  $\approx$  2) pathways.<sup>43,55</sup> The way in which these silica-surfactant composites form the mesophase structures, and the stage in the reaction where the silica-surfactant molecular interactions become important are, however, not yet fully understood.

The mechanism suggested by the inventors of MCM-41 and related phases for their formation is the liquid crystal templating (LCT) mechanism.<sup>18</sup> This proposes that the structure of the channel systems in these mesoporous materials is determined by the surfactant aggregation behaviour, rather than the condensation of the silica around the template molecule, as occurs for zeolites. Exactly how the silica and surfactant interact in the system is still, however, under debate. Beck *et al.*<sup>18</sup> proposed two alternate mechanisms in which the surfactant might self-assemble into the observed silica-surfactant composite structures.

The first mechanism (Figure 1.3(a)) posited the existence of a hexagonally ordered, concentrated surfactant phase, prior to the addition of the silicate to the system. Upon silicate addition, the anions entered the water regions between adjacent micelles in this pre-existing phase and condensed in these interstitial sites without greatly perturbing the surfactant structure. The second mechanism (Figure 1.3(b)) required only that some surfactant micelles be present in the solution prior to the addition of the silicate anions. It was not necessary that the surfactant already exist in the hexagonal liquid crystal phase observed in the final product. In this case, upon the addition of silica to the system, silicate anions coated the surface of the surfactant micelles by some form of ion-exchange with the surfactant counterion. These silica encased micelles then self-ordered to form the hexagonal phase observed in the final product, and condensation of the silicate occurred to freeze in this structure.

Much work was then carried out to distinguish these mechanisms. In the form of the preparation frequently used to obtain hexagonal phase composite silica-surfactant material, the concentration of the surfactant used (10-26 wt%) is far below the concentration where the hexagonal phase would normally form, even at room temperature. Addition of the silicate anion to the system appears to move the phases which occur normally for the templating surfactant to lower concentrations,<sup>43</sup> despite the fact that the cmc would usually increase for increasing counterion radius and pH. The cmc would however be expected to decrease with increases in the valency of the counterions and the ionic strength of the solution.<sup>65</sup> Evidence from small angle neutron scattering,<sup>71,72</sup> X-ray scattering,<sup>73</sup> scanning and transmission electron microscopy<sup>74</sup> and  $^2H$ ,  $^{29}Si$ <sup>75</sup> and  $^{14}N$ <sup>37</sup> nmr also show that no hexagonal phase surfactant structures exist prior to the addition of the silicate, favouring the second mechanism suggested above. It has also been shown that varying the silicate concentration at constant surfactant concentration will result in the formation of hexagonal, lamellar and cubic phases, implying a prominent structure directing role for the inorganic silicate anions in this system.<sup>44</sup>



There are, however a few examples in the literature where very high concentrations of surfactant have been used to create a surfactant liquid crystal phase,<sup>43,76</sup> into which monomeric silicate anions were then introduced. Condensation of the silica in these phases led to the formation of monolithic rigid silica-surfactant composites with structures the same as those of the original surfactant phase. This approach however, appears only to work with very high concentration surfactant systems under conditions where the silicate condensation and consequent release of small molecules do not greatly perturb the existing surfactant structure.

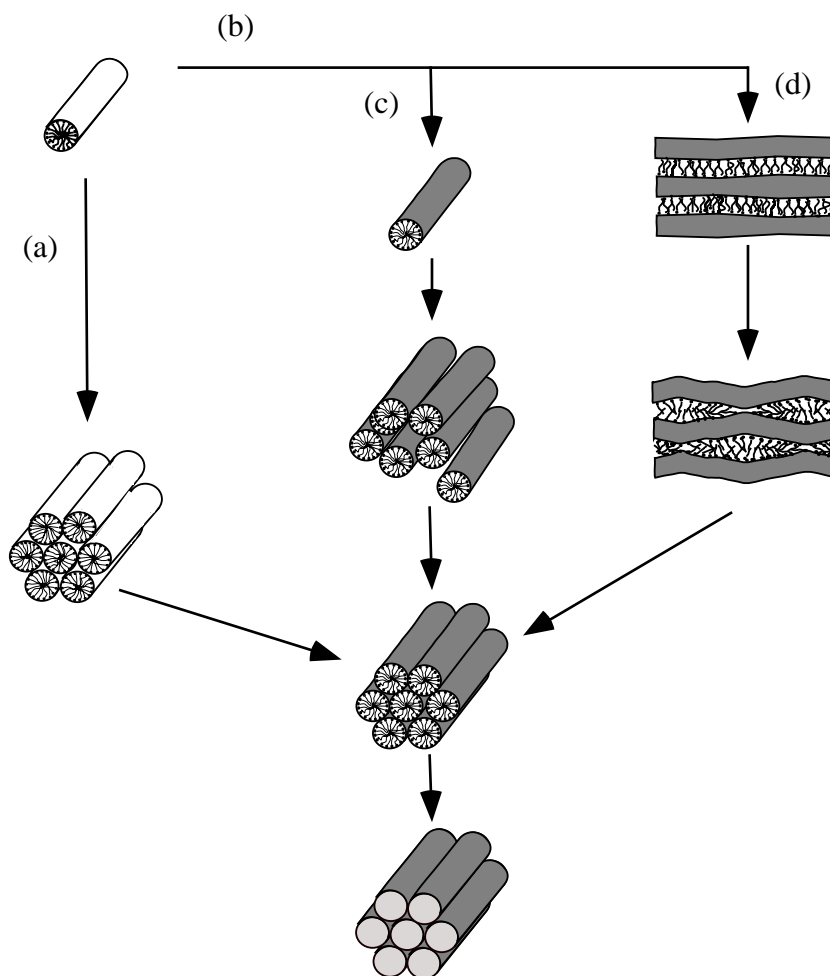


**Figure 1.3** Schematic showing various suggested mechanisms for the formation of MCM-41 as referred to in the text. The change in micelle colour from white to grey indicates the coating of the micelle headgroups with silicate oligomers which results in either (a) an unperturbed cast of the pre-existing surfactant liquid crystal phase, (b) the formation of silica coated surfactant species which form either (c) micelles which then agglomerate to form ordered and disordered arrays or (d) a lamellar phase when converts into the final hexagonal phase material. The final step, calcination results in an array of hollow, hexagonally packed tubes.

In preparations using lower surfactant concentrations, two further refinements of the second micellar-assembly mechanism have been suggested. Several groups have observed the formation of a lamellar silica-surfactant phase in the early stages of preparations which subsequently formed hexagonal phase MCM-41.<sup>37,47,63,77</sup> This observation, led them to propose a “charge density matching” reaction scheme,<sup>37,63</sup>

(Figure 1.3(c)) in which surfactant monomers or micelles in solution become coated with silica oligomers, which act as multidentate ligands for the headgroups of the surfactant. The charge on these oligomers will probably cause the surfactant micelle to alter shape during the ion-exchange process. The screening of the electrostatic double-layer repulsion among the aggregates, by the silicate coating, then induces self-assembly of the ordered mesophases. The mesophase formed, by analogy with the surfactant packing parameter discussed in section 1.2 above, will be that with the least curvature which is consistent with the surfactant, pH and silicate concentration. These two processes - the coating of the micelle and the self-assembly of the mesophase occur on a similar time scale. With the subsequent condensation of the silicate, the inorganic charge density decreases, and lower surfactant charge densities are needed to stabilise the structure, and so the headgroup area per surfactant molecule increases. This increase in headgroup area drives a phase change, for example from lamellar to hexagonal, which is possible since the incompletely condensed silicate walls are still sufficiently flexible to undergo the thinning which this entails. In this model, the wall thickness is determined by the double-layer potential - silica is only accumulated at the interface to the extent necessary for charge compensation. This results in wall thicknesses of 10-11 Å for lamellar phases, and 8-9 Å for hexagonal phases, as observed.<sup>47</sup> Post-synthesis treatment in water at 100°C with pH = 7-10 of various silica-surfactant phases, made with different surfactants, also show phase changes consistent with changes in charge density due to increasing silica condensation and wall reconstruction.<sup>48</sup> A detailed scheme based on the free energy of the various interactions contributing to the synthesis process in this reaction scheme has been proposed.<sup>47,55,63</sup>

Other workers however, do not observe the formation of a lamellar phase as a precursor to hexagonal phase formation.<sup>78-80</sup> In fact, at room temperature in one preparation where a lamellar phase is initially present, the subsequent formation of the hexagonal phase does not occur as a direct transformation but proceeds via the dissolution of the lamellar phase followed by crystallisation of the hexagonal phase.<sup>81</sup> Evidence from transmission electron microscopy, which shows hexagonal phase MCM-41 where a significant proportion of the crystal edges meet at 120°, led Cheng *et al.*<sup>74</sup> to propose a different pathway (Figure 1.3(d)). In this mechanism, the silicate anion first reacts with the pre-existing surfactant micelle, enabling formation of rods of silicated surfactant species. These then self-assemble directly into the hexagonal phase, via the formation of small hexagonal clusters. These clusters are enormous molecular groups which have faces that may grow at different rates, due to inhomogeneities in concentration in the surrounding synthesis gel. Adjacent faces are however more likely to be in the same solution environment, allowing the 120° angle between the neighbouring edges of the resultant crystal to be preserved. This mechanism allows for the formation of both perfect and imperfect crystal shapes, depending on the homogeneity of the reaction medium. Formation of the hexagonal phase via a lamellar phase is unlikely to produce 120° angles between crystal faces. The formation of a wide range of macroscopic morphologies made up from mesoporous silica in a silica/surfactant system seen using scanning electron microscopy has also been explained by an accretion of silicated micelles mechanism.<sup>52</sup> It is suggested that the growth patterns observed are characteristic of a system which is far from equilibrium and not necessarily described by a free energy function.

Packing arguments have also been put forwards for this direct assembly of silicated rods mechanism.<sup>82</sup> They suggest that it is difficult to see how a transformation from a lamellar phase to a multidimensional phase like the cubic phase would occur. All of the mesophases can, however, be considered as various forms of packing of silicated rods - the lamellar phase being caused by packing rods directly on top of each other, and the cubic by intertwined rods. Other evidence for the direct formation of hexagonal phase material from silicated rod structures is given by transmission electron microscopy. Micrographs show areas of randomly oriented tubes of the same dimensions as those in hexagonally packed areas within the same MCM-41 crystal. In this case, imperfect packing of the silica-coated rod-like micelles leads to the formation of the randomly oriented phase.<sup>78</sup> Also, work done using cryo-TEM at very early stages of the MCM-41 preparation has detected clusters of highly elongated, partially silicated micelles with dimensions similar to the correlation lengths seen in small angle X-ray scattering from the same solution.<sup>73</sup> As the reaction proceeds, silica covers more of each micelle and penetrates into them, causing the decrease in intermicellar distance from *ca.* 50 Å to that observed in hexagonal phase MCM-41, *ca.* 40 Å. The formation of these micelles from the pre-existing spherical surfactant micelles in solution is explained using curvature arguments, as were used above. The headgroup repulsion between surfactant molecules is decreased by the presence of silica anions, which increases the curvature of the micelle by decreasing the headgroup area, and promotes formation of longer micelles, which then form clusters.

In this mechanism the driving force for the reaction is both the energetically favourable organic-inorganic interactions and entropic gain from binding of the silicate anions to the micelles, which displaces a layer of ordered water surrounding the micelle. It has been predicted that organic species which do not cause the organisation of water will not act as templates in this system.<sup>35</sup> *In situ* <sup>14</sup>N nmr has shown no evidence of hexagonal surfactant phases in the synthesis media during MCM-41 formation. Rather, the results were consistent with randomly ordered rod-like micelles coated with a silica sheath which did not perturb the motion of the nitrogen containing surfactant headgroups.<sup>78</sup> This result also favours the direct formation of the hexagonal phase from these silicated micelles. Work on the catalytic effect of the surfactant micelles upon silica condensation also suggests the direct assembly of silicated rod-like micelles into the hexagonal phase when monomeric silica at ambient temperatures is used in the preparation. It was, however, also acknowledged that the precise mechanism might strongly depend upon the silica source or reaction conditions (particularly temperature).<sup>5</sup>

As an interesting comparison, the mechanism of formation of the other hexagonally ordered mesoporous silicate is noted. This material is formed by the intercalation of a surfactant into the layered polysilicate kanemite and is called FSM-16 (from Folded Sheet Mechanism, where the number refers to the length of the carbon chain used in the intercalating surfactant).<sup>83</sup> Kanemite consists of single layered silica sheets of linked silica tetrahedra with hydrated sodium ions in the interlayers.<sup>84</sup> The first step in FSM-16 formation is the ion-exchange of a cationic surfactant ion for the Na<sup>+</sup> between the layers. The second step is the folding and condensation of the silicate into a three-

dimensional silicate framework through an interlayer cross-linking process.<sup>85</sup> There may be some breaking up of the layers of kanemite at this stage with local reordering of the silica tetrahedra within the layer occurring.<sup>86</sup> The synthetic conditions for formation of FSM-16 are milder than those for MCM-41, occurring at 70°C and requiring only low surfactant concentrations (3.2 wt%). The silicate walls are more condensed in these materials than in MCM-41 and they retain the particle morphology of the initial polysilicate, indicating substantial differences from the LCT materials.<sup>86</sup> Much greater disorder has been seen in the packing of channels in FSM-16, by electron microscopy, than in MCM-41 materials. It has been suggested that FSM-16 may contain pores which are not straight or long, but are likely to be interconnected in a three dimensional network.<sup>86</sup> No cubic phase has been synthesised from these materials. However, the mechanism is still driven by the aggregation of surfactant ions which is induced by the higher concentration of ions between the silicate layers. This is similar to the lamellar → hexagonal phase mechanism described above.

One report has been made concerning the heterogenous nucleation of MCM-41. In that work, the presence of colloidal particles was shown to promote the formation of hexagonal phase mesopores in a system which otherwise produced amorphous silica.<sup>87</sup> When colloidal silica was used, the colloidal particles formed sites for initial aggregation of silica-surfactant composites. The particle then slowly dissolved and was converted into well ordered, hexagonal phase material, growing in towards the centre of the particle. The presence of more colloidal material induced greater long range order in the product. When colloidal titania which did not dissolve during the reaction, was used, well ordered mesoporous silicates again nucleated on the surface. This ordering is probably due to the adsorption of the surfactant species on the particle surface and probably shares some features with the mechanisms of formation of thin films of MCM-41 on mica,<sup>88</sup> and at the air-water interface.<sup>89,90</sup>

In the present work, aging experiments and *in situ* heating experiments on synthesis gels were carried, out in order to determine the evolution of the formation of MCM-41 in the particular system under study. Investigation of the silica-surfactant species, under conditions where micelles were not present, was done using monomolecular films of surfactant on a Langmuir trough. The ability of the silica-surfactant hexagonal phase to align under shear or to decompose into silica coated rod-like micelles which would align was also investigated. Some conclusions concerning the mechanism of hexagonal phase MCM-41 formation were drawn from this work, described in Chapter 4.

## 1.6 Applications of MCM-41

Applications of MCM-41 largely turn on its large, monodisperse and adjustable pore sizes, and its high surface areas and pore volumes. In its aluminosilicate form it has been shown to be mildly acidic,<sup>91</sup> and its hydrophobicity can be altered by changing the Si/Al ratio. Materials containing more silica are more hydrophobic.<sup>92,93</sup> It is relatively thermally stable, however in the presence of moisture may undergo hydrolysis causing breakdown of the pore structure on time scales of 6 to 18 months (see Chapter 4).

Many suggestions have been made for possible uses of MCM-41.<sup>18,61,65</sup> Catalytic processes such as the processing of high distillates of crude oils into more valuable products,<sup>60</sup> and the synthesis of large molecules are frequently mentioned. The MCM-41 materials in this case would be either substituted with various catalytically active transition metal oxides, either in whole or in part, or else would act as inert, high surface area supports for catalytic entities bound to the walls of the channels. Some shape-selection may possibly arise from the shape of the pores by analogy with zeolites. It has been shown that the narrow pore size distribution of these materials promotes catalytic activity for the production of dimethylacetals, over materials with broader pore size distributions.<sup>94</sup>

Aluminosilicate MCM-41 materials have been shown to be moderately good catalysts for the cracking of large organic molecules to smaller ones. The activity generally increases with increasing aluminium content.<sup>91</sup> Comparisons with commercial fluid catalytic cracking catalysts has shown that AlMCM-41, for a given conversion, gives higher amounts of gaseous products, indicating more severe cracking, and yields more olefins and lower amounts of branched hydrocarbons.<sup>95</sup> Many patents and papers mention the catalytic use of AlMCM-41 for acid catalysis, and TiMCM-41 and VMCM-41 for liquid redox catalysis, and these have been reviewed.<sup>65,95</sup> These conclude that the improvement observed over conventional catalysts is often due to higher surface areas and increased accessibility of active sites, although much work still is required on regeneration, and behaviour under realistic working conditions before industrial usage will be feasible.<sup>95</sup>

Some workers have reported incorporation of catalysts such as 2,4,6-triphenylpyrylium<sup>96</sup> (for isomerisation of *cis*-stilbene) and  $[\text{Pt}_{15}(\text{CO})_{30}]^{2-}$  (in FSM-16 channels for catalysis in the water gas shift reaction)<sup>97</sup> via ship-in-a-bottle syntheses inside mesoporous silica channels. Molecules of titanocene dichloride have been diffused into the MCM-41 pores and grafted to the walls via reactions with the pendant silanol groups. These were then converted to isolated titania species by calcination, with the resulting materials proving to have a very high turnover frequency for the epoxidation of alkenes.<sup>98</sup> Many other molecules especially organometallics have been directly adsorbed into the MCM-41 pores and anchored, by various methods of grafting, to the walls.<sup>96,99-104</sup> These often prove to have good catalytic activity for various reactions including the production of highly isotactic polypropene,<sup>100</sup> the conversion of low-density polyethylene into hydrocarbon feedstocks,<sup>105</sup> alkene oxidation<sup>101,103</sup> and the formation of fine chemicals which involve bulky reactants or products.<sup>94,104</sup> Catalytic activity has also been observed for aluminosilicate MCM-41 ion-exchanged

with sodium and caesium cations.<sup>106</sup> Organically modified MCM-41 materials with possible catalytic applications have also been directly prepared in one-step syntheses by neutral templating routes which allow the template to be removed by washing rather than by calcination.<sup>107</sup>

The channels of MCM-41 have also been used to create nanosized metal clusters of platinum by various methods,<sup>108,109</sup> NiMo oxides,<sup>110</sup> caesium-lanthanum oxides<sup>111</sup> and Fe<sub>2</sub>O<sub>3</sub><sup>112</sup> by incipient wetness techniques. The materials containing platinum nanocrystals were shown to be good catalysts for the oxidation of CO, with samples prepared using the incipient wetness method showing the best performance.<sup>108</sup> They also show high catalytic activity for the hydrogenolysis of ethane,<sup>109</sup> and of branched alkanes.<sup>113</sup> The NiMo impregnated material showed good performance as a catalyst for cracking vacuum gasoil under mild operating conditions.<sup>110</sup> Iron (II) impregnated MCM-41 materials loaded with palladium amine clusters showed some activity in an oxygen-rich environment for breakdown of NO<sub>x</sub> and hydrocarbons present in exhaust gases.<sup>114</sup>

The use of nanoscale fabrication technology within the large pores of these materials has also been suggested, in order to form many other types of composite material. These include the formation of quantum wires through the polymerisation of conducting polymers, or metal complexes encapsulated in the silicate frameworks. Previously quantum wires have been formed by molecular beam epitaxy and atomic layer epitaxy but it is difficult to make structures below diameters of about 100 Å using these methods. Wu and Bein<sup>115,116</sup> have already shown that it is possible to polymerise monomers for conducting polymers, such as polyaniline, within the MCM-41 channels, resulting in conducting filaments lining the mesopores.<sup>117</sup> They have also produced conducting carbon wires inside MCM-41 channels by pyrolysing polyacrylonitrile polymerised inside the pores. Previous work with zeolites had resulted in filaments too small to carry charge, but inside the larger MCM-41 channels, interchain and transverse interactions are permitted, allowing significant conductivity to be observed.<sup>118</sup> Other workers report the polymerisation of styrene,<sup>119</sup> methyl methacrylate, and vinyl acetate<sup>120</sup> within the silica based mesopores. Properties of the encapsulated polymers were different to those in the bulk. Specifically the glass transition temperature was reduced and the molecular weight was inversely dependant on pore size. Ko and Ryoo<sup>121</sup> have manufactured platinum wires within the pore system of MCM-41 by repeated soaking in Pt(NH<sub>3</sub>)<sub>4</sub>(NO<sub>3</sub>)<sub>2</sub> solutions, followed by drying and reduction to metallic platinum. These wires were used to image individual channels via transmission electron microscopy.

Separation and adsorption applications such as protein separations and the selective adsorption of large organic molecules from waste water are also frequently proposed. Pure silica zeolite analogues exhibit a high efficiency in selectively adsorbing organic pollutants from waste waters. Increased pore sizes might extend this usage of pure silica frameworks, to filter out larger molecules such as polychlorinated biphenyls or herbicide and pesticide molecules in drinking water.<sup>122</sup> MCM-41 with its monodisperse, ordered pores which may be varied in size, has been put forward as a model mesoporous adsorbent for the testing of theories of adsorption of small

molecules such as nitrogen, argon, oxygen and water in porous systems.<sup>123-127</sup> MCM-41 materials with varied pore sizes have been used to test models for the diffusion of glucose and glucitol in water.<sup>128</sup>

The steep rise in adsorption at certain value of  $P/P_0$ , caused by the sudden filling of mesopores with water vapour, in a pure silica MCM-41 has been shown to be function of the pore size. This effect is reproducible, and reversible and the MCM-41 substrate is stable over several cycles. This has led to the suggestion that such mesoporous materials be used in the design and fabrication of humidity sensors.<sup>93</sup>

The structuring observed in these mesoporous materials is of a length scale where quantum confinement of the electronic states, related to the pore size, could be expected, and so porous metal oxides made in this fashion should also possess altered electronic properties. Porous materials made from semiconducting metal oxides may be able to be used as sensors, if their electronic surface states react to the adsorption of the substance to be detected.<sup>66</sup> Use of porous transition-metal oxide systems for applications in non-linear optics, such as molecular sieves for electronic and optical applications,<sup>65</sup> and as thermal or acoustic insulation have also been suggested.<sup>68</sup>

In the early literature, including patents, MCM-41 has been put forward as having possible uses in drug delivery systems,<sup>61</sup> and as even being able to encapsulate proteins in ultra-large pore materials. Confining such difficult to crystallise molecules in a rigid lattice may create an ordering matrix to allow structure determination by X-ray diffraction.<sup>129</sup> The large number of pendant hydroxyl groups lining the inside surface of MCM-41 also suggests the possibility of anchoring enzymes to the interior surfaces. These enzymes would then be situated in precisely defined chemical environments, and could be used for the commercial production of biological molecules.<sup>130</sup> Surfactant templating techniques have been used to create porous calcium oxide (aragonite) and calcium phosphate structures similar to those found in the skeletons of marine algae.<sup>131,132</sup> This points to the possibility of considerable application of such techniques in the field of biomineralisation, to create artificial bone, or shell or to mimic the structure of natural organic-inorganic composites optimised for a particular task.

Since many of these applications utilise the high surface area and relative stability of MCM-41 materials, it becomes important to have a detailed knowledge of the structure of the material in order that its properties may be optimised for various applications. Uses such as the testing of theoretical models of adsorption require a good model of the molecular potentials which make up the wall surfaces. The optimisation of binding of catalytically active complexes, or the formation of molecular wires or nanosize particles of other materials within the channels will benefit greatly from a molecular level structure. Work on the structure and wall characteristics of pure silica MCM-41 is reported in Chapters 5 and 5. Data from a number of techniques, small angle X-ray and neutron scattering, quasielastic neutron scattering from molecules adsorbed in the MCM-41 channels, gas adsorption isotherms, and X-ray and neutron diffraction have been combined to determine a detailed model of the wall structure of these materials.

## 1.7 References

1. E.M. Flanigen, *Pure & Appl. Chem.*, **1980**, 52, 2191-2211.
2. C.J. Brinker and G.W. Scherer, *Sol-Gel Science. The Physics and Chemistry of Sol-Gel Processing*, Academic Press, San Diego, **1990**.
3. H.E. Bergna in *The Colloid Chemistry of Silica*; Advances in Chemistry Series, (Ed. H.E. Bergna), American Chemical Society, Washington D.C., **1994**, Vol. 243, 1-47.
4. D.H. Olson, *J. Phys. Chem.*, **1970**, 74, 2758-2764.
5. C.-F. Cheng, Z. Luan and J. Klinowski, *Langmuir*, **1995**, 11, 2815-2819.
6. S.L. Suib, *Chem. Rev.*, **1993**, 93(2), 803-826.
7. W.O. Haag in *Zeolites and Related Microporous Materials: State of the Art 1994*; Studies in Surface Science and Catalysis, (Eds. J. Weitkamp, H.G. Karge, H. Pfeifer and W. Hölderich), Elsevier Science B.V., **1994**, Vol. 84, 1375-1394.
8. R.M. Dessau, J.L. Schlenker and J.B. Higgins, *Zeolites*, **1990**, 10, 522-524.
9. M.E. Davis, C. Saldarriaga, C. Montes, J. Garces and C. Crowder, *Nature*, **1988**, 331, 698-699.
10. R.H. Jones, J.M. Thomas, J. Chen, R. Xu, Q. Huo, S. Li, Z. Ma and A.M. Chippindale, *J. Solid State Chem.*, **1993**, 102, 204-208.
11. P.B. Moore and J. Shen, *Nature*, **1983**, 306, 356-358.
12. L.W. Hrubesh, *Chem. & Ind.*, **1990**, 17 December, 824-827.
13. T.J. Pinnavaia in *Materials Chemistry: An Emerging Discipline*; Advances in Chemistry Series, (Eds. L.V. Interrante, L.A. Carper and A.B. Ellis), ACS, Washington D.C., **1995**, Vol. 245, 283-300.
14. P.E. Sokol, R.T. Azuah, M.R. Gibbs and S.M. Bennington, *J. Low Temp. Phys.*, **1996**, 103(1/2), 23-33.
15. T. Dabadie, A. Ayrat, C. Guizard, L. Cot and P. Lacan, *J. Mater. Chem.*, **1996**, 6(11), 1789-1794.
16. H.F. Poulsen, J. Neuefeind, H.-B. Neumann, J.R. Schneider and M.D. Zeidler, *J. Non-Cryst. Solids*, **1995**, 188, 63-74.
17. A.C. Wright, *J. Non-Cryst. Solids*, **1994**, 179, 84-115.
18. J.S. Beck, J.C. Vartuli, W.J. Roth, M.E. Leonowicz, C.T. Kresge, K.D. Schmitt, C.T.-W. Chu, D.H. Olson, E.W. Sheppard, S.B. McCullen, J.B. Higgins and J.L. Schlenker, *J. Am. Chem. Soc.*, **1992**, 114, 10834-10843.
19. D.H. Everett, *Pure Appl. Chem.*, **1972**, 31, 578.
20. E.J.P. Feijen, J.A. Martens and P.A. Jacobs in *Zeolites and Related Microporous Materials: State of the Art 1994*; Studies in Surface Science and Catalysis, (Eds. J. Weitkamp, H.G. Karge, H. Pfeifer and W. Hölderich), Elsevier Science B.V., **1994**, Vol. 84, 3-20.
21. S.L. Burkett and M.E. Davis, *Chem. Mater.*, **1995**, 7(5), 920-928.
22. M.E. Davis and R.F. Lobo, *Chem. Mater.*, **1992**, 4, 756.
23. S.P. Zhdanov in *Molecular Sieve Zeolites - I*; Advanced in Chemistry Series, (Eds. E.M. Flanigen and L.B. Sand), ACS, Washington D.C., **1971**, Vol. 101, 20-43.
24. G.T. Kerr, *J. Phys. Chem.*, **1966**, 1047.
25. R.M. Barrer, J.W. Baynham and F.W. Bultide, *J. Chem. Soc.*, **1959**, 195.
26. M. Wiebcke and D. Hoebbel, *J. Chem. Soc., Dalton Trans.*, **1992**, 2451-2455.



27. R.M. Barrer, *Hydrothermal Chemistry in Zeolites*, Academic Press, London, **1982**.
28. J.J. Keijsper and M.F.M. Post in *Zeolite Synthesis*; ACS Symposium Series, (Eds. M.L. Occelli and M.E. Robson), ACS, Washington D.C., **1989**, Vol. 398, 28-48.
29. C.T.G. Knight, *Zeolites*, **1990**, 10, 140-144.
30. B.D. McNicol, G.T. Pott, K.R. Loos and N. Mulder in *Molecular Sieves*; Advances in Chemistry Series, (Eds. W.M. Meier and J.B. Uytterhoeven), ACS, Washington D.C., **1973**, Vol. 121, 152-161.
31. W.H. Dokter, H.F. van Garderen, T.P.M. Beelen, R.A. van Santen and W. Bras, *Angew. Chem. Int. Ed. Engl.*, **1995**, 34(1), 73-75.
32. A. Culfaz and L.B. Sand in *Molecular Sieves*; Advances in Chemistry Series, (Eds. W.M. Meier and J.B. Uytterhoeven), ACS, Washington D.C., **1973**, Vol. 121, 140-151.
33. F. DiRenzo, F. Remoue, P. Massiani, F. Fajula, F. Figueras and T. Des Courières in *Molecular Sieves - Synthesis of Microporous Material*; (Eds. M.L. Occelli and H.E. Robson), Van Nostrand Reinhold, New York, **1992**, Vol. 1, 115-128.
34. J.C. Jansen, C.W.R. Engelen and H. van Bekkum in *Zeolite Synthesis*; (Eds. M.L. Occelli and H.E. Robson), ACS, Washington D.C., **1989**, Vol. 398, 257-273.
35. M.E. Davis, C.-Y. Chen, S.L. Burkett and R.F. Lobo in *Mat. Res. Soc. Symp. Proc. "Better Ceramics Through Chemistry VI"*; "Better Ceramics Through Chemistry IV", (Eds. C.J.B. A. K. Cheetham M. L. Mecartney and C. Sanchez), Materials Research Society, Pittsburg, PA, **1994**, Vol. 346, 831-842.
36. J.S. Beck, J.C. Vartuli, G.J. Kennedy, C.T. Kresge, W.J. Roth and S.E. Schramm, *Chem. Mater.*, **1994**, 6, 1816-1821.
37. A. Firouzi, D. Kumar, L.M. Bull, T. Besier, P. Sieger, Q. Huo, S.A. Walker, J.A. Zasadzinski, C. Glinka, J. Nicol, D. Margolese, G.D. Stucky and B.F. Chmelka, *Science*, **1995**, 267, 1138-1143.
38. Y. Chevalier and T. Zemb, *Rep. Prog. Phys.*, **1990**, 53, 279-371.
39. G.J.T. Tiddy, *Physics Reports*, **1980**, 57(1), 1-46.
40. J.N. Israelachvili, *Surfactants in Solution*, Plenum, New York, **1987**.
41. J.N. Israelachvili, D.J. Mitchell and B.W. Ninham, *J. Chem. Soc., Faraday Trans. 2*, **1976**, 72, 1527.
42. J.N. Israelachvili in *Physics of Amphiphiles: Micelles, Vesicles and Microemulsions*; (Ed. X.C. Corso), Soc. Italiana di Fisica, Bologna, **1985**, 24-58.
43. N.K. Raman, M.T. Anderson and C.J. Brinker, *Chem. Mater.*, **1996**, 8(8), 1682-1701.
44. J.C. Vartuli, K.D. Schmitt, C.T. Kresge, W.J. Roth, M.E. Leonowicz, S.B. McCullen, S.D. Hellring, J.S. Beck, J.L. Schlenker, D.H. Olson and E.W. Sheppard, *Chem. Mater.*, **1994**, 1994(6), 2317-2326.
45. L.M. Bull, D. Kumar, S.P. Millar, T. Besier, M. Janicke, G.D. Stucky and B.F. Chmelka in *Zeolites and Related Microporous Materials: State of the Art 1994*; Stud. Surf. Sci. Catal., (Eds. J. Weitkamp, H.G. Karge, H. Pfeifer and W. Hölderich), Elsevier Science B.V., **1994**, Vol. 84A, 429-434.

46. M. Dubois, T. Gulik-Krzywicki and B. Cabane, *Langmuir*, **1993**, 9(3), 673-680.
47. A. Monnier, F. Schüth, Q. Huo, D. Kumar, D. Margolese, R.S. Maxwell, G.D. Stucky, M. Krishnamurty, P. Petroff, A. Firouzi, M. Janicke and B.F. Chmelka, *Science*, **1993**, 261, 1299-1303.
48. Q. Huo, D.I. Margolese and G.D. Stucky, *Chem. Mater.*, **1996**, 8(5), 1147-1160.
49. P.T. Tanev and T.J. Pinnavaia, *Science*, **1996**, 271, 1267-1269.
50. A. Chenite, Y. Le Page, V.R. Karra and A. Sayari, *J. Chem. Soc., Chem. Commun.*, **1996**, 413-414.
51. S. Schacht, Q. Huo, I.G. Voigt-Martin, G.D. Stucky and F. Schüth, *Science*, **1996**, 273, 768-771.
52. H. Yang, N. Coombs and G.A. Ozin, *Nature*, **1997**, 386, 692-695.
53. Q. Huo, J. Feng, F. Schüth and G.D. Stucky, *Chem. Mater.*, **1997**, 9(1), 14-17.
54. S.A. Davis, S.L. Burkett, N.H. Mendelson and S. Mann, *Nature*, **1997**, 385, 420-423.
55. Q. Huo, D.I. Margolese, U. Ciesla, D.G. Demuth, P. Feng, T.E. Gier, P. Sieger, A. Firouzi, B.F. Chmelka, F. Schüth and G.D. Stucky, *Chem. Mater.*, **1994**, 6, 1176-1191.
56. S.A. Bagshaw, E. Prouzet and T.J. Pinnavaia, *Science*, **1995**, 269, 1242-1244.
57. P.T. Tanev and T.J. Pinnavaia, *Science*, **1995**, 267, 865-867.
58. J.S. Beck, C.T.-W. Chu, I.D. Johnson, C.T. Kresge, M.E. Leonowicz, W.J. Roth and J.C. Vartuli, *US Patent, No. 5,108, 725*, **1992**.
59. C.T. Kresge, M.E. Leonowicz, W.J. Roth, J.C. Vartuli and J.S. Beck, *Nature*, **1992**, 359, 710-712.
60. C.T. Kresge, M.E. Leonowicz, W.J. Roth and J.C. Vartuli, *US Patent, No. 5,102,643*, **1992**.
61. C.T. Kresge, M.E. Leonowicz, W.J. Roth and J.C. Vartuli, *US Patent No. 5,098,684*, **1992**.
62. D. Khushalani, A. Kuperman, N. Coombs and G.A. Ozin, *Chem. Mater.*, **1996**, 8(8), 2188-2193.
63. G.D. Stucky, A. Monnier, F. Schüth, Q. Huo, D. Margolese, D. Kumar, M. Krishnamurty, P. Petroff, A. Firouzi, M. Janicke and B.F. Chmelka, *Mol. Cryst. Liq. Cryst.*, **1994**, 240, 187-200.
64. D. Khushalani, A. Kuperman, G.A. Ozin, K. Tanaka, J. Garcés, M.M. Olken and N. Coombs, *Adv. Mater.*, **1995**, 7(10), 842-846.
65. X.S. Zhao, G.Q. Lu and G.J. Millar, *Ind. Eng. Chem. Res.*, **1996**, 35(7), 2075-2090.
66. P. Behrens, *Angew. Chem. Int. Ed. Engl.*, **1996**, 35(5), 515-518.
67. Q. Huo, D.I. Margolese, U. Ciesla, P. Feng, T.E. Gier, P. Sieger, R. Leon, P.M. Petroff, F. Schüth and G.D. Stucky, *Nature*, **1994**, 368, 317-321.
68. D.M. Antonelli and J.Y. Ying, *Chem. Mater.*, **1996**, 8(4), 874-881.
69. D.M. Antonelli and J.Y. Ying, *Angew. Chem. Intl. Ed. Engl.*, **1996**, 35(4), 426-430.
70. D.M. Antonelli, A. Nakahira and J.Y. Ying, *Inorg. Chem.*, **1996**, 35(11), 3126-3136.
71. C.J. Glinka, J.M. Nicol, G.D. Stucky, E. Ramli, D. Margolese, Q. Huo, J.B. Higgins and M.E. Leonowicz, *J. Porous Materials*, **1996**, 3, 93-98.

72. L. Auvray, A. Ayrat, T. Dabadie, L. Cot, C. Guizard and J.D.F. Ramsay, *Faraday Discuss.*, **1995**, *101*, 235-247.
73. O. Regev, *Langmuir*, **1996**, *12*(20), 4940-4944.
74. C.-F. Cheng, H. He, W. Zhou and J. Klinowski, *Chem. Phys. Lett.*, **1995**, *244*, 117-120.
75. W. Kolodziejcki, A. Corma, M.-T. Navarro and J. Pérez-Pariente, *Solid State Nuclear Magnetic Resonance*, **1993**, *2*, 253-259.
76. G.S. Attard, J.C. Glyde and C.G. Göltner, *Nature*, **1995**, *378*, 366-368.
77. A. Steel, S.W. Carr and M.W. Anderson, *J. Chem. Soc., Chem Commun.*, **1994**, 1571-1572.
78. C.Y. Chen, S.L. Burkett, H.-X. Li and M.E. Davis, *Microporous Mater.*, **1993**, *2*, 22.
79. S. O'Brien, R.J. Francis, S.J. Price, D. O'Hare, S. Clark, N. Okazaki and K. Kuroda, *J. Chem. Soc., Chem. Commun.*, **1995**, 2423-2424.
80. A. Ortlam, J. Rathousky, G. Schulz-Ekloff and A. Zukal, *Microporous Mater.*, **1996**, *6*(4), 171-180.
81. A. Matijasic, A.-C. Voegtlin, J. Patarin, J.L. Guth and L. Huve, *J. Chem. Soc., Chem. Commun.*, **1996**, 1123-1124.
82. J.C. Vartuli, K.D. Schmitt, C.T. Kresge, W.J. Roth, M.E. Leonowicz, S.B. McCullen, S.D. Hellring, J.S. Beck, J.L. Schlenker, D.H. Olson and E.W. Sheppard in *Zeolites and Related Microporous Materials: State of the Art 1994.*; Stud. Surf. Sci. Catal., (Eds. J. Weitkamp, H.G. Karge, H. Pfeifer and W. Hölderich), Elsevier Science B.V., **1994**, *Vol. 84A*, 53-60.
83. S. Inagaki, Y. Fukushima and K. Kuroda in *Zeolites and Related Microporous Materials: State of the Art 1994.*; Stud. Surf. Sci. Catal., (Eds. J. Weitkamp, H.G. Karge, H. Pfeifer and W. Hölderich), Elsevier Science B.V., **1994**, *Vol. 84A*, 125-132.
84. K. Kuroda, *J. Porous Mater.*, **1996**, *3*, 107-114.
85. S. Inagaki, A. Koiwai, N. Suzuki, Y. Fukushima and K. Kuroda, *Bull. Chem. Soc. Jpn.*, **1996**, *69*(5), 1449-1457.
86. C.-Y. Chen, S.-Q. Xiao and M.E. Davis, *Microporous Mater.*, **1995**, *4*(1), 1-20.
87. J. Liu, A.Y. Kim, J.W. Virden and B.C. Bunker, *Langmuir*, **1995**, *11*(3), 689-692.
88. H. Yang, A. Kuperman, N. Coombs, S. Mamiche-Afara and G.A. Ozin, *Nature*, **1996**, *379*, 703-705.
89. H. Yang, N. Coombs, I. Sokolov and G.A. Ozin, *Nature*, **1996**, *381*, 589-592.
90. I.A. Aksay, M. Trau, S. Manne, I. Honma, N. Yao, L. Zhou, P. Fenter, P.M. Eisenberger and S.M. Gruner, *Science*, **1996**, *273*, 892-898.
91. R. Mokaya, W. Jones, Z. Luan, M.D. Alba and J. Klinowski, *Catal. Lett.*, **1996**, *37*, 113-120.
92. P.L. Llewellyn, F. Schüth, Y. Grillet, F. Rouquerol and K.K. Unger, *Langmuir*, **1995**, *11*, 574-577.
93. S. Komarneni, R. Pidugu and V.C. Menon, *J. Porous Mater.*, **1996**, *3*, 99-106.
94. M.J. Climent, A. Corma, S. Iborra, M.C. Navarro and J. Primo, *J. Catal.*, **1996**, *161*, 783-789.
95. A. Sayari, *Chem. Mater.*, **1996**, *8*(8), 1840-1852.

96. A. Corma, V. Fornés, H. García, M.A. Miranda and M.J. Sabater, *J. Am. Chem. Soc.*, **1994**, *116*(21), 9767-9768.
97. T. Yamamoto, T. Shido, S. Inagaki, Y. Fukushima and M. Ichikawa, *J. Am. Chem. Soc.*, **1996**, *118*(24), 5810-5811.
98. T. Maschmeyer, F. Rey, G. Sankar and J.M. Thomas, *Nature*, **1995**, *378*, 159-162.
99. S. O'Brien, J. Tudor, S. Barlow, M.J. Drewitt, S. Heyes and D. O'Hare, *J. Chem. Soc., Chem. Commun.*, **1997**, 641-642.
100. J. Tudor and D. O'Hare, *J. Chem. Soc., Chem. Commun.*, **1997**, 603-604.
101. C.-J. Liu, S.-G. Li, W.-Q. Pang and C.-M. Che, *J. Chem. Soc., Chem. Commun.*, **1997**, 65-66.
102. P. Sutra and D. Brunel, *J. Chem. Soc., Chem. Commun.*, **1996**, 2485-2486.
103. R. Burch, N. Cruise, D. Gleeson and S.C. Tsang, *J. Chem. Soc., Chem. Commun.*, **1996**, 951-952.
104. I.V. Kozhevnikov, A. Sinnema, R.J.J. Jansen, K. Pamin and H. van Bekkum, *Catal. Letts.*, **1995**, *30*, 241-252.
105. J. Aguado, D.P. Serrano, M.D. Romero and J.M. Escola, *J. Chem. Soc., Chem. Commun.*, **1996**, 725-726.
106. K.R. Kloetstra and H. van Bekkum, *J. Chem. Soc., Chem. Commun.*, **1995**, 1005-1006.
107. D.J. Macquarrie, *J. Chem. Soc., Chem. Commun.*, **1996**, 1961-1962.
108. U. Junges, W. Jacobs, I. Voigt-Martin, B. Krutzsch and F. Schüth, *J. Chem. Soc., Chem. Commun.*, **1995**, 2283-2284.
109. R. Ryoo, C.H. Ko, J.M. Kim and R. Howe, *Catal. Lett.*, **1996**, *37*, 29-33.
110. A. Corma, A. Martínez, V. Martínez-Soria and J.B. Montón, *J. Catal.*, **1995**, *153*, 25-31.
111. K.R. Kloetstra, M. van Laren and H. van Bekkum, *J. Chem. Soc., Faraday Trans.*, **1997**, *93*(6), 1211-1220.
112. T. Abe, Y. Tachibana, T. Uematsu and M. Iwamoto, *J. Chem. Soc., Chem. Commun.*, **1995**, 1617-1618.
113. T. Inui, J.-B. Kim and M. Seno, *Catal. Lett.*, **1994**, *29*, 271-279.
114. P.P. Paul, M.A. Miller, M.J. Heimrich and S.T. Schwab in *Microporous and Macroporous Materials*; Mat. Res. Soc. Symp. Proc., (Eds. R.F. Lobo, J.S. Beck, S.L. Suib, D.R. Corbin, M.E. Davis, L.E. Iton and S.I. Zones), MRS, Pittsburgh, **1995**, *Vol. 431*, 117-122.
115. C.-G. Wu and T. Bein in *Zeolites and Related Microporous Materials: State of the Art 1994.*; Stud. Surf. Sci. Catal., (Eds. J. Weitkamp, H.G. Karge, H. Pfeifer and W. Hölderich), Elsevier Science B.V., **1994**, *Vol. 84A*, 243-250.
116. C.-G. Wu and T. Bein, *Chem. Mater.*, **1994**, *6*, 1109-1112.
117. C.-G. Wu and T. Bein, *Science*, **1994**, *264*, 1757-1759.
118. C.-G. Wu and T. Bein, *Science*, **1994**, *266*, 1013-1015.
119. H.L. Frisch and J.E. Mark, *Chem. Mater.*, **1996**, *8*(8), 1735-1738.
120. P.L. Llewellyn, U. Ciesla, R. Stadler, F. Schüth and K.K. Unger in *Zeolites and Related Microporous Materials: State of the Art 1994.*; Stud. Surf. Sci. Catal., (Eds. J. Weitkamp, H.G. Karge, H. Pfeifer and W. Hölderich), Elsevier Science B.V., **1994**, *Vol. 84A*, 2013-2020.
121. C.H. Ko and R. Ryoo, *J. Chem. Soc., Chem. Commun.*, **1996**, 2467-2468.

122. P. Behrens, *Adv. Mater.*, **1993**, 5(2), 127-132.
123. O. Franke, G. Schulz-Ekloff, J. Rathousky, J. Stárek and A. Zukal, *J. Chem. Soc., Chem. Commun.*, **1993**, 724-725.
124. P.J. Branton, P.G. Hall and K.S.W. Sing, *J. Chem. Soc., Chem Commun.*, **1993**, 1257-1258.
125. P.J. Branton, P.G. Hall, K.S.W. Sing, H. Reichert, F. Schüth and K.K. Unger, *J. Chem. Soc., Faraday Trans.*, **1994**, 90(19), 2965-2967.
126. P.J. Branton, PhD Thesis, University of Exeter, **1994**.
127. R. Schmidt, M. Stöcker, E. Hansen, D. Akporiaye and O.H. Ellestad, *Microporous Mater.*, **1995**, 3(4/5), 443-448.
128. R. Netrabukkana, K. Lourvanij and G.L. Rorrer, *Ind. Eng. Chem. Res.*, **1996**, 35(2), 458-464.
129. Z. Blum and S.T. Hyde, *Acta Chemica Scandinavica*, **1994**, 48, 88-90.
130. J.M. Thomas, *Nature*, **1994**, 368, 289-290.
131. D. Walsh and S. Mann, *Nature*, **1995**, 377, 320-323.
132. D. Walsh and S. Mann, *Chem. Mater.*, **1996**, 8(8), 1944-1953.